Implementation and Experimental Validation of a Photovoltaic-Thermal (PVT) Collector Model in TRNSYS

Danny Jonas[1], Danjana Theis[2] and Georg Frey[1]

[1] Saarland University, Chair of Automation and Energy Systems, Saarbrücken (Germany)

[2] htw saar, University of Applied Sciences, Saarbrücken (Germany)

Abstract

Photovoltaic-thermal (PVT) collectors are hybrid solutions for solar collectors converting solar energy in electrical and thermal energy. To figure out best solutions and new possibilities for the application of PVT collectors, system simulations are often used as first step before proving in real applications. At this, the development of well-validated PVT collector models is an important task. This contribution presents the implementation of a performance model for the electrical part of PVT collectors in TRNSYS, which can be coupled to existing models of solar thermal collectors for the simulation of hybrid PVT collectors, and first results of the model validation with experimental measurements of three different PVT collectors. Furthermore, a parameter identification process with TRNSYS and GenOpt for a coupled PVT collector model is introduced and described in detail. In addition, a comparison of the electrical model with a four-parameter (single diode) PV model is presented to figure out if its implementation will improve the accuracy of the simulation results. The presented results pointed out that the PVT model in combination with the proposed parameter identification process achieves a good agreement of simulated and measured thermal and electrical power output for the analyzed PVT collector types and operating conditions.

Keywords: modeling, simulation, photovoltaic-thermal collectors, experimental validation, TRNSYS

1. Introduction

Photovoltaic-thermal (PVT) collectors are hybrid solutions for solar collectors converting solar energy in electrical and thermal energy. The main objective of these hybrid system combinations is to use the large part of unused solar energy in conventional photovoltaic (PV) modules for thermal applications. The thermal coupling of solar thermal absorbers to the solar PV cells results in a thermal energy harvesting system for PV cells. For fluid temperature conditions below the operating temperature of conventional PV modules, the thermal coupling and heat transfer of the thermal solar energy to a heat carrier leads additionally to a cooling of the PV modules and thus to a reduction of the PV cell temperature. As the electrical efficiency of PV modules also depends on the module temperature and increases with decreasing cell temperature, the coupling leads to higher PV performance in combined thermal and electrical operation of the PVT collectors. Especially for applications in buildings, the available roof and wall area is often a limiting factor for the use of PV and solar thermal energy and both systems compete with each other for this area. Depending on the PVT collector type and application, e.g. for the use in heat pump heating systems, the use of PVT collectors counteracts this competition and can lead to a better utilization of the available area and a maximized overall solar yield.

The availability of many different types of PVT collectors on the market necessitates a classification of PVT collector types based on the used technological approaches. In general, PVT collectors can be classified into liquid-based PVT, air-based PVT or others, like PCM-based PVT, depending on the used heat transfer carrier medium. Regarding the design of the collector, PVT collectors are often classified in WISC (wind and/or infrared sensitive collectors, often referred to as ‘uncovered’), covered or concentrating collectors. One possibility to further distinguish between special types of WISC or covered PVT collectors is the classification into collectors with backside thermal insulation or without backside thermal insulation (and in case of WISC also retrofit PVT collectors).

To figure out best solutions and new possibilities for the application of different types of PVT collectors, system simulations are often used as first step before proving in real applications. At this, the development of well-validated PVT collector models is an important task to analyze different configurations and designs of energy systems with PVT collector integration in system simulations. In 2018, the International Energy Agency Solar Heating and Cooling

doi:10.18086/eurosun2018.02.16 Available at http://proceedings.ises.org

Nomenclature

Abbreviations

GPS	generalized pattern search
HJ	Hooke-Jeeves
IAM	incidence angle modifier
IEA	International Energy Agency
ISO	International Organization for Standardization
MPP	maximum power point
NOCT	nominal operating cell temperature
PCM	phase change material
PSO	particle swarm optimization
PV	photovoltaic
PVT	photovoltaic-thermal
SHC	solar heating and cooling
STC	standard test conditions
WISC	wind and/or infrared sensitive collectors

Symbols

A	gross area, m²
a	model parameter a for irradiance dependence of PV efficiency calculation, m² W^{-1}
b_0	constant for incident angle modifier IAM, -
c_1	heat loss coefficient, W m^{-2}K^{-1}
c_2	temperature dependence of the heat loss coefficient, W m^{-2}K^{-2}
c_3	wind speed dependence of the heat loss coefficient, J m^{-3}K
c_4	sky temperature dependence of the heat loss coefficient, -
c_5	effective thermal capacity, J m^{-2}K
c_6	wind speed dependence of the zero loss efficiency, s m^{-1}
b	model parameter b for irradiance dependence of PV efficiency calculation, -
c	model parameter c for irradiance dependence of PV efficiency calculation, -
E_L	long wave irradiance in PVT plane, W m^{-2}
G	global solar irradiance in PVT plane, W m^{-2}
G_d	diffuse solar irradiance in PVT plane, W m^{-2}
I	current, A
K_b	IAM for direct radiation, -
K_d	IAM for diffuse radiation, -
$\dot{m}$	mass flow rate, kg h^{-1}
$\mathrm{MAE_{el}}$	mean absolute error of the electrical power output, W
$\mathrm{MAE_{th}}$	mean absolute error of the thermal power output, W
$\mathrm{nMAE_{el}}$	normalized mean absolute error of the electrical power output, -
$\mathrm{nMAE_{th}}$	normalized mean absolute error of the thermal power output, -
$\mathrm{nRMSE_{el}}$	normalized root mean square error of the electrical power output, -
$\mathrm{nRMSE_{th}}$	normalized root mean square error of the thermal power output, -
p_abs	absolute pressure of the ambient air, Pa
P_el	electrical power output of PVT collector, W
p_el	specific electrical power output of PVT collector, W m^{-2}
PR	performance ratio, -
Q_th	thermal energy output of PVT collector, kWh
$\dot{Q}_\mathrm{th}$	thermal power output of PVT collector, W
$\dot{q}_\mathrm{th}$	specific thermal power output of PVT collector, W m^{-2}
RH	relative humidity, %
$\mathrm{RMSE_{el}}$	root mean square error of the electrical power output, W
$\mathrm{RMSE_{th}}$	root mean square error of the thermal power output, W
T	temperature, °C
t	time, h
V	voltage, V
W_el	electrical energy output of PVT collector, kWh
u	wind speed in the PVT plane, m s^{-1}
$U_{\mathrm{cell-fl}}$	internal heat transfer coefficient from PV cell to fluid, W m^{-2} K^{-1}
β	power temperature coefficient of the PV cells, % K^{-1}
η_0	zero loss collector efficiency, -
η_el	overall electrical efficiency of the PVT collector, -
θ	incidence angle of beam radiation, °
σ	the Stefan-Boltzmann constant, W m^{-2}K^{-4}

Subscripts

cell	cell
el	electrical
G	global solar irradiance
in	inlet
IAM	incidence Angle Modifier
m	mean
meas	measurement
ref	reference (usually STC) conditions
sim	simulation
out	outlet
T	temperature
th	thermal
tot	total, overall

Programme initiated a new task on the application of PVT collectors (IEA SHC Task 60), which focus on the application of PVT collectors with the aim to assess existing solutions and to develop new system solutions with advantages in comparison to classical 'side by side installations' of PV and solar thermal collectors (IEA SHC, 2018). One objective of IEA SHC Task 60 is also to improve the performance characterization and modeling of PVT collectors and systems, which pointed out the need for the development of well-validated PVT simulation models.

Within the research project SolWP-Hybrid, different types of PVT collectors (WISC, covered, with and without backside thermal insulation) will be investigated by simulation and on a test bench for the application in solar thermal and heat pump systems. This contribution presents the implementation of a performance model for the electrical part of PVT collectors in TRNSYS (Type 835: PV model for the coupling with solar thermal absorber and collector models as PVT model), which is based on the work of Lämmle et al. (2017), and first results of the model validation with experimental measurements including the parameter identification procedure. In addition, a comparison of the model results for the electrical part of crystalline modules of the implemented performance model with an adapted standard four-parameter (single diode) PV model in TRNSYS will be presented. The intention of this comparison is to figure out if the implementation of a four-parameter PV model in the developed TRNSYS Type 835 will improve the accuracy of the electrical performance simulation results for crystalline PV modules.

In the following sections, the PVT collector modelling (section 2) and the experimental measurement (section 3) are described. Afterwards, in section 4 the process and results of the parameter identification with TRNSYS and GenOpt are presented. This is followed by the validation of the model with test sequences and the comparison of the electrical results with an adapted four-parameter PV model (section 5). Finally, section 6 provides the main conclusions and an outlook on further work.

2. PVT collector modelling in TRNSYS

2.1 Overview

The main idea behind this model, which is based on the work of Lämmle et al. (2017), is to develop a PV performance model in TRNSYS, which can be coupled to existing models of solar thermal collectors or absorbers for the calculation of the electrical power output of WISC and covered PVT collectors (see Fig. 1). It is especially developed for the connection with thermal models which are based on the quasi-dynamic model of ISO 9806:2013 (ISO 9806, 2013) or ISO 9806:2017 (ISO 9806, 2017), e.g. TRNSYS Type 832 (Haller et al., 2013).

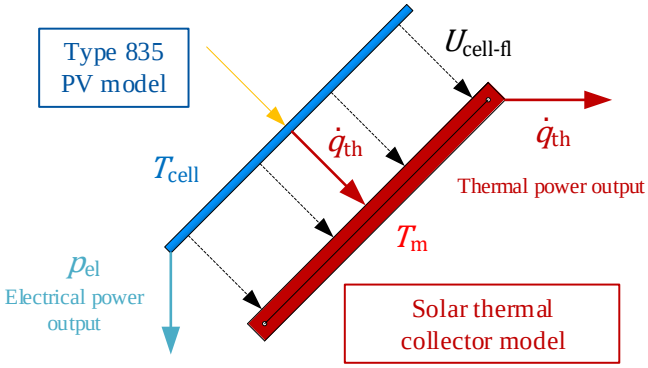

Fig. 1 Coupled PVT model

As addition, the model includes a PV mode to simulate PV modules based on the same performance model, e.g. for a comparison of the electrical yield of a PV module and PVT collectors using identical PV cells. The major difference between the calculation of PV modules and PVT collectors in this approach results from the cell temperatures, which are determined by the fluid temperature in PVT collectors and by a steady-state module temperature in PV modules.

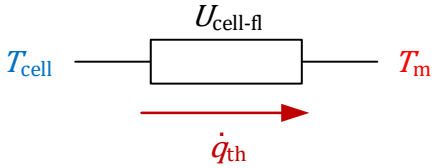

Fig. 2 Thermal network

In case of PVT collectors, the PVT cell temperature T_{cell} is calculated via an equivalent thermal network with an internal heat transfer coefficient $U_{\text{cell-fl}}$, which connects the PVT cell temperature with the mean fluid temperature T_{m} of the PVT collector (see Fig. 2), according to the electrical performance model of Lämmle et al. (2017). In case of PV modules, the PV cell temperature is calculated by the Faiman model (Faiman, 2008) or from NOCT conditions. As this contribution focus on PVT collectors, the PV modes of Type 835 are not described in detail.

2.1 Electrical model

Overall electrical efficiency and electrical power output

The overall (or total) electrical efficiency η_{el} of the PVT collector is calculated with:

$$\eta_{\text{el}} = \eta_{\text{el,ref}} \cdot PR_{\text{tot}} \qquad \text{(eq. 1)}$$

The electrical power output of the PVT collector P_{el} is given by:

$$P_{\text{el}} = \eta_{\text{el,ref}} \cdot PR_{\text{tot}} \cdot G \cdot A_{\text{PVT}} \qquad \text{(eq. 2)}$$

and as specific electrical power output by (Lämmle et al., 2017):

$$p_{\text{el}} = \eta_{\text{el,ref}} \cdot PR_{\text{tot}} \cdot G \qquad \text{(eq. 3)}$$

where $\eta_{\text{el,ref}}$ is the electrical efficiency at reference conditions (usually STC conditions), PR_{tot} is the overall instantaneous performance ratio, G the global radiation on PVT plane and A_{PVT} the PVT collector area.

The overall instantaneous performance ratio is calculated with (Lämmle et al., 2017):

$$PR_{\text{tot}} = PR_{\text{IAM}} \cdot PR_{\text{T}} \cdot PR_{\text{G}} \qquad \text{(eq. 4)}$$

The electrical performance model takes into account the following loss effects (performance ratios PR):

- loss effects of incidence angle PR_{IAM}
- loss effects of irradiance PR_{G} and
- PV cell temperature dependence of electrical efficiency PR_{T}.

Loss effects of incidence angle

The instantaneous performance ratio due to incidence angle losses PR_{IAM} is calculated with (Duffie and Beckman, 2013):

$$PR_{\mathrm{IAM}} = 1 - b_{0,\mathrm{el}} \cdot [1/\cos(\theta) - 1] \quad \text{(eq. 5)}$$

where $b_{0,\mathrm{el}}$ is the constant for electrical IAM and θ the incidence angle of beam radiation.

Loss effects of irradiance

The instantaneous performance ratio due to irradiance losses PR_{G} is calculated with (Heydenreich et al., 2008):

$$PR_{\mathrm{G}} = a \cdot G + b \cdot \ln(G+1) + c \cdot \left[\left(\ln(G+\mathrm{e})\right)^2/(G+1) - 1\right] \quad \text{(eq. 6)}$$

with the model parameters a in m² W^{-1}, b and c dimensionless, the global irradiance G in W m^{-2} and the Euler's number e.

PV cell temperature dependence of the electrical efficiency

The PV cell temperature dependence of the electrical efficiency is calculated with (Skoplaki and Palyvos, 2009):

$$PR_{\mathrm{T}} = 1 - \beta \cdot (T_{\mathrm{cell}} - T_{\mathrm{ref}}) \quad \text{(eq. 7)}$$

where β is the power temperature coefficient of the PV cells, T_{cell} the temperature of the PV cells and T_{ref} the PV cell temperature at reference conditions (usually STC conditions).

PVT cell temperature

The PVT cell temperature is calculated with a simple equivalent thermal network with an internal heat transfer coefficient $U_{\mathrm{cell-fl}}$, which connects the PVT cell temperature T_{cell} with the mean fluid temperature T_{m} of the PVT collector. The mean fluid temperature is calculated as mean temperature between the thermal model input and output temperature (in this contribution Type 832). The PVT cell temperature is then given by (Lämmle et al., 2016, 2017):

$$T_{\mathrm{cell}} = T_{\mathrm{m}} + \dot{q}_{\mathrm{th}}/U_{\mathrm{cell-fl}} \quad \text{(eq. 8)}$$

where $\dot{q}_{\mathrm{th}}$ is the specific thermal power output of the PVT collector.

2.2 Thermal model

The thermal performance of PVT collectors can be described with the following quasi-dynamic collector model, which is implemented in TRNSYS Type 832 and is also described in ISO 9806:2013 (and with two additional terms in ISO 9806:2017):

$$\dot{q}_{\mathrm{th}} = \eta_0 \cdot (K_{\mathrm{b}} \cdot G_{\mathrm{b}} + K_{\mathrm{d}} \cdot G_{\mathrm{d}}) - c_1 \cdot (T_{\mathrm{m}} - T_{\mathrm{a}}) - c_2 \cdot (T_{\mathrm{m}} - T_{\mathrm{a}})^2 - c_3 \cdot u \cdot (T_{\mathrm{m}} - T_{\mathrm{a}}) + c_4 \cdot \left(E_{\mathrm{L}} - \sigma \cdot {T_{\mathrm{a}}}^4\right) - c_5 \cdot \mathrm{d}T_{\mathrm{m}}/\mathrm{d}t - c_6 \cdot u \cdot G \quad \text{(eq. 9)}$$

with

$$K_{\mathrm{b}} = 1 - b_{0,\mathrm{th}} \cdot [1/\cos(\theta) - 1] \quad \text{(eq. 10)}$$

where $\dot{q}_{\mathrm{th}}$ is the specific thermal power output of the PVT collector, η_0 the zero loss collector efficiency, K_{b} the IAM for direct radiation, K_{d} the IAM for diffuse radiation, c_1 the heat loss coefficient, c_2 the temperature dependence of the heat loss coefficient, c_3 the wind speed dependence of the heat loss coefficient, u the wind speed in the PVT plane, c_4 the sky temperature dependence of the heat loss coefficient, E_{L} the long-wave irradiance, σ the Stefan-Boltzmann constant, c_5 the effective thermal capacity, c_6 the wind speed dependence of the zero loss efficiency, $b_{0,\mathrm{th}}$ the constant for thermal IAM and θ the incidence angle of beam radiation. As the electrical mode of operation has a significant impact on the thermal efficiency, the thermal performance coefficients for the thermal power output calculation of the PVT collector should be determined in MPP mode (Lämmle et al., 2017).

3. Experimental measurements

The experimental measurements of the PVT collectors were realized in July and August 2018 on an outdoor test bed in Saarbrücken (Germany) at the Laboratory for Solar Energy Systems of the University of Applied Sciences htw saar. Three different types of PVT collectors:

- PVT A - WISC
- PVT B - covered, with backside thermal insulation
- PVT C - covered, without backside thermal insulation

are installed on a test roof and are monitored under dynamic outdoor conditions during MPP operation. Beside of the standard measurements of the thermal performance according to ISO 9806:2017, the relevant electrical values are measured continuously. A systematic scheme of the measurement including the main measured values which are used for the performance characterization of the PVT collectors is shown in Fig. 3. Due to measurement problems, the long-wave irradiation is recalculated for the parameter identification and model validation by the use of a calculated view temperature between ambient and sky temperature (calculated with the ambient air temperature, ambient air pressure and the relative humidity). According to ISO 9806:2017, the following typical days should be included in the quasi dynamic test of the collector performance:

- Day Type 1: η_0-conditions, mostly clear sky conditions
- Day Type 2: elevated operating temperature or η_0-conditions, partly cloudy conditions including broken cloud and clear sky conditions
- Day Type 3: mean operating temperature conditions including clear sky conditions
- Day Type 4: high operating temperature conditions including clear sky conditions.

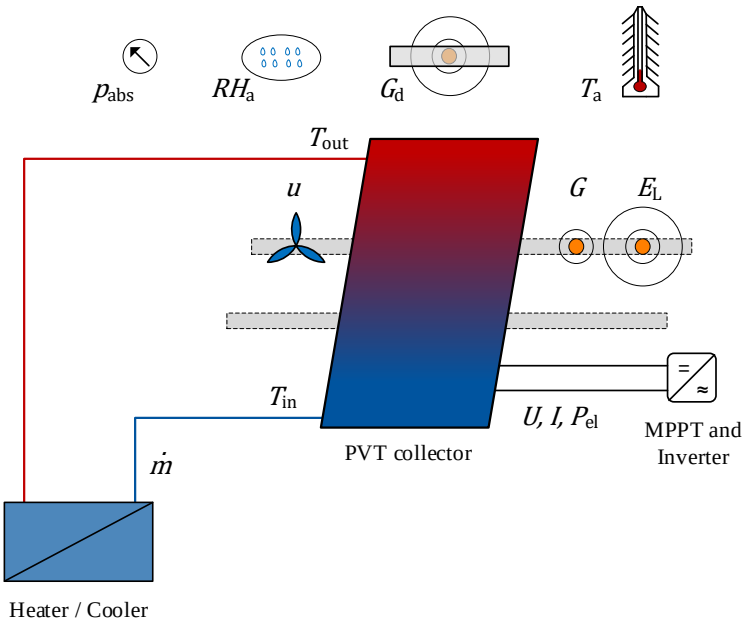

Fig. 3: Measurement scheme of the outdoor test

For the identification of the PVT collector model parameters, the measured test data was evaluated and usable test sequences were chosen for combined test sequences with all four day types. Within the combined test sequences, a Boolean value is defined as indicator if the time step should be taken into account for the parameter identification or not. The objective of this process is the filtering of start-up sequences between the different sequences and bad data, e.g. if something was changed in the test bed or measured values are outside a reliable or usable range.

4. Parameter identification with GenOpt

Identification or determination of model parameters by comparing and adjusting simulated results to measured data is a well-known procedure for different applications, especially in the field of solar thermal systems. In general, a

cost function is defined to assess the agreement of the model results with the measured data. The model parameters are then adjusted to better fit the measurement by minimization of the cost function. In the field of solar thermal collectors and systems, the most common methods for the minimization process are multiple linear regression (MLR), which has been introduced as extended version by Perers (1997), and dynamic parameter identification with the fit program DF (Spirkl, 1997) which use the Levenberg-Marquardt algorithm (Fischer et al., 2012). Furthermore, newer approaches like Budig et al. (2009) or Almeida (2014) use GenOpt (Wetter, 2016) in combination with TRNSYS for the parameter identification process. GenOpt is a generic optimization program to minimize a cost function that is evaluated by an external simulation program like TRNSYS and includes a library with local and global one-dimensional and multi-dimensional optimization algorithms, like Particle Swarm Optimization (PSO, meta-heuristic population-based algorithm, stochastic) or Hooke-Jeeves algorithm (GPS-HJ, generalized pattern search method, deterministic).

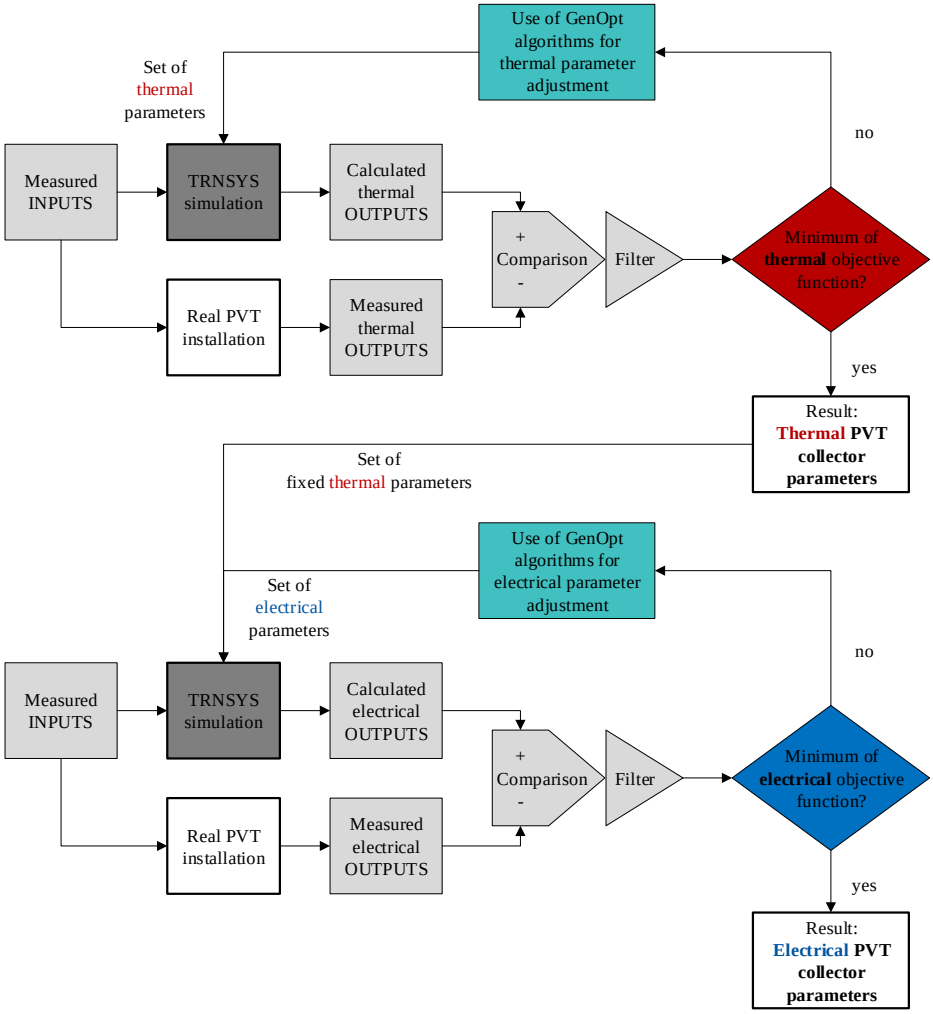

Fig. 4: Model parameter identification process

The proposed parameter identification process with TRNSYS and GenOpt for the PVT collector model is shown in Fig. 4. A set of measured values is used as time dependent input for the TRNSYS simulation via a data reader. The measured inputs (E_L, G, G_d, θ, T_a, RH_a, p_abs, u, $\dot{m}$, T_in) are then used to calculate the thermal and electrical outputs of the TRNSYS model, especially the thermal $\dot{Q}_\mathrm{th,sim}$ and the electrical $P_\mathrm{el,sim}$ power output of the PVT collector. Subsequently, the calculated thermal outputs are compared via the absolute error and filtered with the Boolean function described in chapter 3. This is followed by the calculation of the thermal cost function which has to be minimized. At this, GenOpt is used to adjust the thermal collector parameters (η_0, K_d, $b_\mathrm{0,th}$, c_1- c_6) until the minimum of the thermal cost function is reached. The identified thermal parameters are then used as fixed parameters and the process is repeated for the electrical parameter identification of $U_\mathrm{cell-fl}$ and $b_\mathrm{0,el}$.

In this work, the mean absolute error (MAE) of the thermal power output is used as cost function for the thermal parameter identification:

$$\mathrm{MAE_{th}} = \frac{1}{n \cdot \Delta t} \sum_{i=1}^{n} \left(\left| \dot{Q}_\mathrm{th,sim} - \dot{Q}_\mathrm{th,meas} \right| \cdot \Delta t \right) \qquad \text{(eq. 11)}$$

and the MAE of the electrical power output for the electrical parameter identification:

$$\mathrm{MAE_{el}} = \frac{1}{n \cdot \Delta t} \sum_{i=1}^{n} \left(\left| P_{\mathrm{el,sim}} - P_{\mathrm{el,meas}} \right| \cdot \Delta t \right) \quad \text{(eq. 12)}$$

The results of the parameter identification of the three different PVT collectors by the use of TRNSYS 17 (TRNSYS, 2015), GenOpt 3.1 (Wetter, 2016), GPS-HJ and MAE as cost function are summarized in Tab. 1. At this, the $\mathrm{MAE_{th}}$ is between 13.18 W and 16.79 W and the $\mathrm{MAE_{el}}$ between 2.93 W and 5.58 W.

Tab. 1: Results of the parameter identification with GPS-HJ algorithm and MAE as cost function

Parameter	Unit	PVT A - WISC	PVT B - covered w/o insulation	PVT C - covered w/ insulation
		Manufacturer and calculated data		
A_{PVT}	m²	1.66	1.79	1.79
$\eta_{\mathrm{el,ref}}$	-	0.1688	0.1406	0.1390
β	%/K	0.467	0.370	0.370
		Identified PVT parameter		
$\eta_{0,\mathrm{th}}$	-	0.436	0.596	0.573
K_{d}	-	0.91	0.93	0.94
$b_{0,\mathrm{th}}$	-	0.114	0.122	0.120
c_1	W/m²K	7.750	6.583	5.008
c_2	W/m²K²	0.026	0.021	0.059
c_3	Ws/m³K	1.640	0.000	0.011
c_4	-	0.000	0.066	0.039
c_5	J/m²K	35800	16075	16631
c_6	s/m	0.008	0.009	0.003
$U_{\mathrm{cell-fl}}$	W/m²K	13.63	15.74	14.07
$b_{0,\mathrm{el}}$	-	0.167	0.182	0.170
		Results of cost functions		
$\mathrm{MAE_{th}}$	W	16.79	13.18	13.22
$\mathrm{MAE_{el}}$	W	5.58	3.04	2.93

5. Model validation and comparison with four-parameter PV model

For the further validation of the TRNSYS model, the PVT collectors are simulated for two sequences (mostly clear sky and partly cloudy) and the model results are compared with the measured values. The dynamic behavior of the thermal and electrical power output of the PVT collector as well as the main solar irradiance data are shown in Fig. 5 for sequence 1 (mostly clear sky, day type 1) and in Fig. 6 for sequence 2 (partly cloudy, day type 2). A summary of the results including the ratio of the difference between the simulated and measured thermal (ΔQ_{th}) or electrical (ΔW_{el}) energy productions related to the measured thermal ($Q_{\mathrm{th,meas}}$) or electrical ($W_{\mathrm{el,meas}}$) energy is given in Tab. 2. For further analysis of the results, the normalized mean absolute errors (nMAEs), the root mean square errors (RMSEs) and the normalized root mean square errors (nRMSEs) are defined as:

$$\mathrm{nMAE_{th}} = \mathrm{MAE_{th}} \,/\, \left[\frac{1}{n \cdot \Delta t} \sum_{i=1}^{n} \left(\dot{Q}_{\mathrm{th,meas}} \cdot \Delta t \right) \right] \quad \text{(eq. 13)}$$

$$\mathrm{nMAE_{el}} = \mathrm{MAE_{el}} \,/\, \left[\frac{1}{n \cdot \Delta t} \sum_{i=1}^{n} \left(P_{\mathrm{el,meas}} \cdot \Delta t \right) \right] \quad \text{(eq. 14)}$$

$$\mathrm{RMSE_{th}} = \sqrt{\frac{\sum_{i=1}^{n} \left[\left(\dot{Q}_{\mathrm{th,sim}} - \dot{Q}_{\mathrm{th,meas}} \right)^2 \cdot \Delta t \right]}{n \cdot \Delta t}} \quad \text{(eq. 15)}$$

$$\mathrm{RMSE_{el}} = \sqrt{\frac{\sum_{i=1}^{n} \left[\left(P_{\mathrm{el,sim}} - P_{\mathrm{el,meas}} \right)^2 \cdot \Delta t \right]}{n \cdot \Delta t}} \quad \text{(eq. 16)}$$

$$\mathrm{nRMSE_{th}} = \mathrm{RMSE_{th}} / \left[\frac{1}{n \cdot \Delta t} \sum_{i=1}^{n} \left(\dot{Q}_{\mathrm{th,meas}} \cdot \Delta t \right) \right] \quad \text{(eq. 17)}$$

$$\mathrm{nRMSE_{el}} = \mathrm{RMSE_{el}} \,/\, \left[\frac{1}{n \cdot \Delta t} \sum_{i=1}^{n} \left(P_{\mathrm{el,meas}} \cdot \Delta t \right) \right] \quad \text{(eq. 18)}$$

Tab. 2: Results of the validation (Day Type 1: 11h15-16h15, Day Type 2: 10h00-14h00)

Parameter	Unit	PVT A - WISC		PVT B - covered w/o insulation		PVT C - covered w/ insulation	
		Day Type 1	Day Type 2	Day Type 1	Day Type 2	Day Type 1	Day Type 2
MAE_{th}	W	10.68	21.32	6.50	21.34	4.59	21.16
$nMAE_{th}$	-	1.79 %	4.39 %	0.73 %	2.89 %	0.51%	2.83%
$RMSE_{th}$	W	13.24	28.61	9.39	33.25	5.96	32.75
$nRMSE_{th}$	-	2.22 %	5.89 %	1.06 %	4.50 %	0.67%	4.38%
$Q_{th,sim}$	kWh	3.034	2.005	4.447	2.971	4.472	2.994
$Q_{th,meas}$	kWh	2.987	1.954	4.430	2.967	4.473	3.005
$\Delta Q_{th}/Q_{th,meas}$	-	+1.58 %	+2.59 %	+0.38 %	+0.15 %	-0.03%	-0.38%
MAE_{el}	W	2.34	3.94	2.11	4.31	1.86	4.04
$nMAE_{el}$	-	1.12 %	2.17 %	1.10 %	2.54 %	0.98%	2.46%
$RMSE_{el}$	W	3.71	6.31	9.73	5.64	2.62	5.36
$nRMSE_{el}$	-	1.77 %	3.48 %	5.07 %	3.32 %	1.39%	3.27%
$W_{el,sim}$	kWh	1.037	0.735	0.970	0.681	0.938	0.656
$W_{el,meas}$	kWh	1.046	0.729	0.961	0.682	0.945	0.660
$\Delta W_{el}/W_{el,meas}$	-	-0.82 %	+0.96 %	+0.98 %	-0.27 %	-0.75%	-0.56%

In case of day type 1, the dynamic behavior shows a good agreement to the measured values of the thermal and electrical power output of the PVT collectors, which is also expressed in a small $nRMSE_{th}$ between 0.67 % and 2.22 % and a $nRMSE_{el}$ between 1.39 % and 5.07 %. The higher $nRMSE_{el}$ of 5.07 % in case of covered PVT B can be explained by a short cut-off of the measured PV power at around 14h45 (possibly a short malfunction of the MPP tracker), which results in higher simulation values during this period. The modeled energy production over the period is also in a good accuracy with a $\Delta Q_{th}/Q_{th,meas}$-ratio between -0.03 % and 1.58 % and a $\Delta W_{el}/W_{el,meas}$-ratio between -0.75 % and +0.98 %.

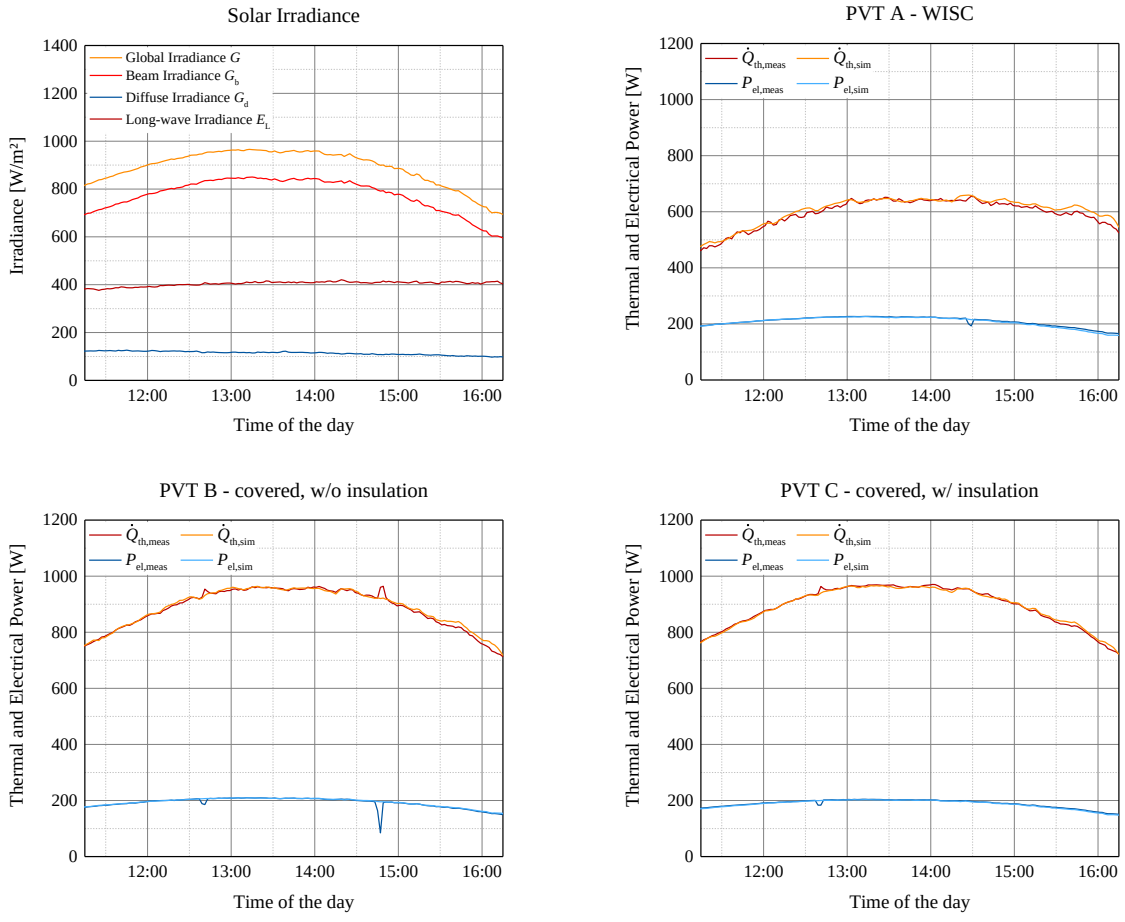

Fig. 5: Model validation – Mostly clear sky (Day Type 1)

For day type 2 with more dynamic behavior of the solar radiation, the differences between the measured and modelled

results are slightly higher with a $nRMSE_{th}$ between 4.38 % and 5.89 % and a $nRMSE_{el}$ between 3.27 % and 3.48 %. However, the modeled energy production over the period is also in a good accuracy with a $\Delta Q_{th}/Q_{th,meas}$-ratio between -0.38 % and 2.59 % and a $\Delta W_{el}/W_{el,meas}$-ratio between -0.56 % and +0.96 %.

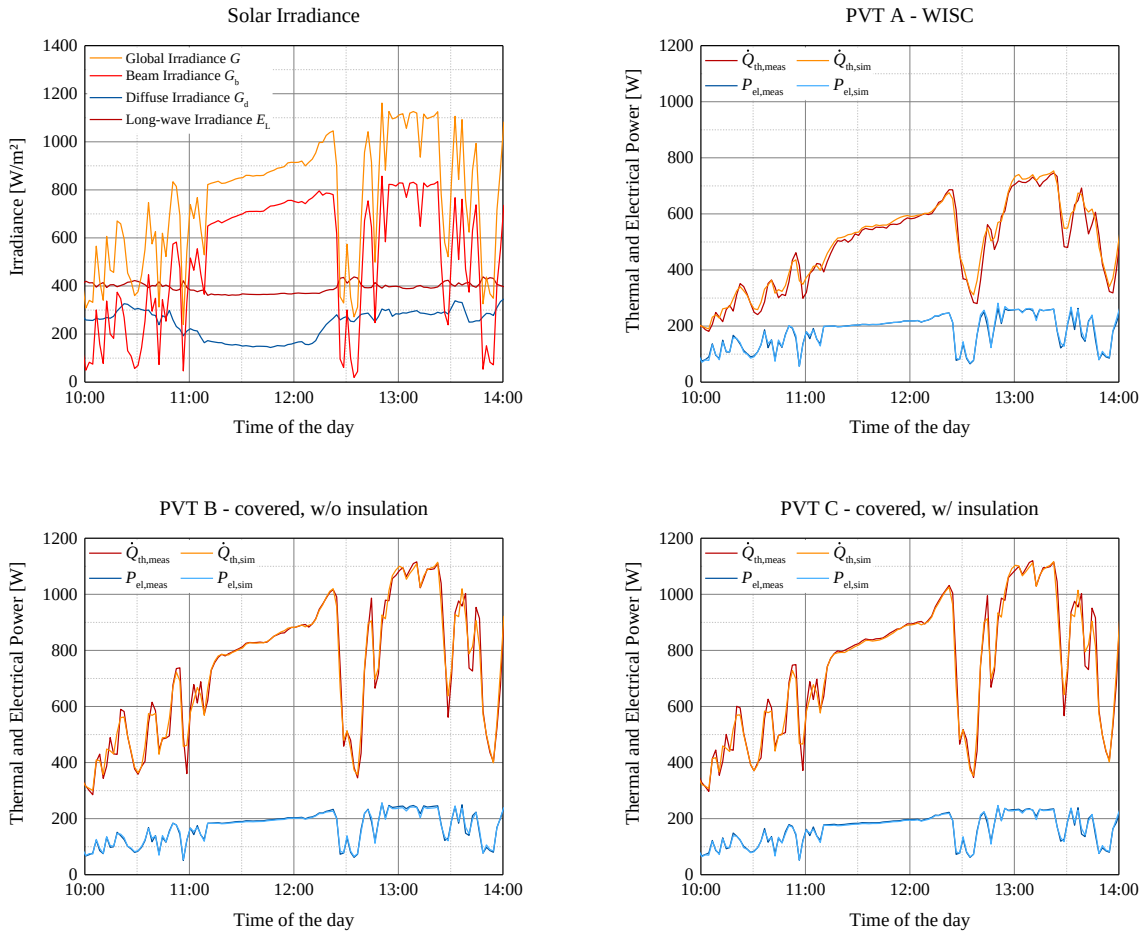

Fig. 6: Model validation – Partly cloudy (Day Type 2)

In general, the electrical results show a better fit of the dynamic behavior then the thermal results, which is expressed in smaller values of $nRMSE_{el}$ (except the short cut-off of PVT B for day type 1). This emphasizes the importance of an accurate fit of the thermal capacity of the PVT collectors. Beside of the thermal capacity effects on the transient behavior, the recalculated long-wave radiation and its inaccuracy could lead to higher values of $nRMSE_{th}$ as it has an impact on the thermal behavior. This is also expressed in a zero c_4-coefficient for the WISC PVT, which usually have higher c_4-coefficents then covered PVT collectors. In further works, it is important to identify the coefficients with a measured long-wave irradiance. As summary, the whole procedure for the PVT model parameter identification with TRNSYS and GenOpt and the model validation is summarized in Fig. 7.

In the following, a comparison of the electrical part of the PVT model with an adapted standard four-parameter (single diode) PV model is presented to figure out if the implementation of a four-parameter PV model in the developed TRNSYS Type 835 will improve the accuracy of the electrical performance results for crystalline PV modules. For the comparison, the standard PV model Type 103 of TRNSYS 18 (TRNSYS, 2018) is recompiled for TRNSYS 17 with extension of the model with the possibility to set the PV cell temperature as input value during the simulation. This allows the usage of the simple equivalent thermal network from section 2 to calculate the PV cell temperature with the internal heat transfer coefficient $U_{cell-fl}$. The parameter identification process is then repeated for the electrical part in combination with the adapted Type 103. For PVT A the result is an internal heat transfer coefficient $U_{cell-fl}$ of 7.88 W/m²K. Afterwards, the PVT collector PVT A is simulated for the two validation sequences (mostly clear sky and partly cloudy) with the different models for the electrical part and the electrical model results are compared with the measured values.

1. Preparing test data for parameter identification
Evaluate test data; Select usable test sequences; Build a combined test sequence with all four day types; Indicate which time steps should be used for the analysis (calculation of cost functions), e.g. for filtering start-up sequences

2. Preparing TRNSYS for parameter identification
Assign measured data files; Set general simulation parameters (e.g. simulation time); Choose special functions like calculating long-wave radiation via effective sky / view temperature if needed

3. Preparing thermal parameter identification
Select cost function (MAE, RMSE) for thermal parameter identification and save TRNSYS input file

4. Thermal parameter identification
Start TRNOPT interface; Select TRNSYS input file; Select and specify thermal parameter variables (start, max, min, step value); Select thermal cost function and optimization method

5. Run thermal parameter identification with GenOpt

6. Select thermal parameter set with minimized cost function

7. Preparing electrical parameter identification
Set identified thermal parameters as fixed parameters in TRNSYS; Select cost function (MAE, RMSE) for electrical parameter identification and save TRNSYS input file

8. Electrical parameter identification
Start TRNOPT interface; Select TRNSYS input file; Select and specify electrical parameter variables; Select electrical cost function and optimization method

9. Run electrical parameter identification with GenOpt

10. Select electrical parameter set with minimized cost function

11. Evaluate results with identified PVT parameters by simulation of validation sequences

Fig. 7: Procedure for PVT model parameter identification with TRNSYS and GenOpt

Fig. 8 shows a comparison of the measured electrical power output ($P_{\mathrm{el,meas}}$) with the model output of Type 835 ($P_{\mathrm{el,835}}$) and the model output of the adapted four-parameter PV model with ($P_{\mathrm{el,4p,Ucorr}}$) and without ($P_{\mathrm{el,4p}}$) correction of $U_{\mathrm{cell-fl}}$. In this case without correction means that the $U_{\mathrm{cell-fl}}$-value from the parameter identification of Type 835 is used instead of the identified value for the adapted four-parameter PV model. A summary of the simulation results is given in Tab. 3.

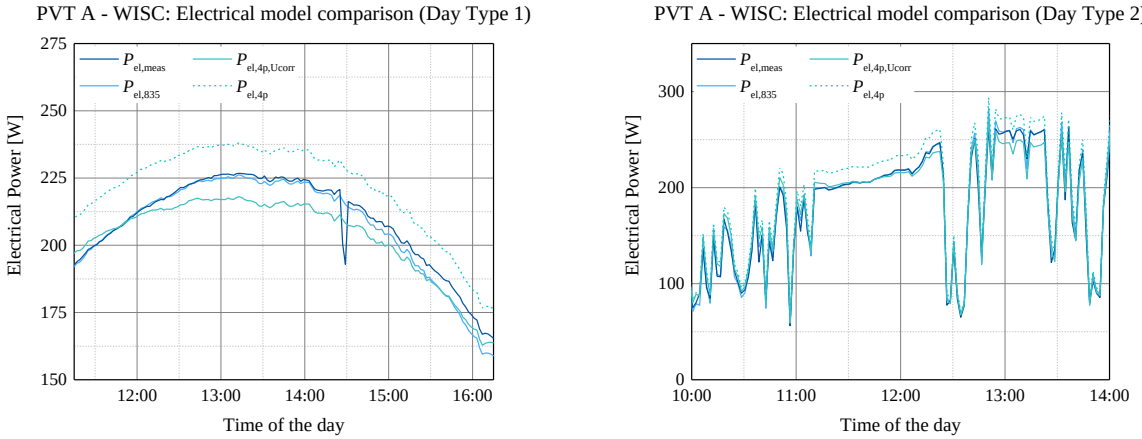

Fig. 8: Electrical model comparison

The results show that the usage of the $U_{\mathrm{cell-fl}}$-value from the parameter identification of Type 835 leads to a high inaccuracy, expressed in $\Delta W_{\mathrm{el}}/W_{\mathrm{el,meas}}$-values between +5.92 % and +7.93 %, $\mathrm{nMAE_{el}}$ up to 7.97 % and $\mathrm{nRMSE_{el}}$ up to 8.70 %. Hence, a new parameter identification is needed if the electrical model is changed. At this, it should be mentioned that the four-parameter PV model is not equipped with a parameter like $b_{0,\mathrm{el}}$ to adjust the incidence angle dependence of the electrical power output to the individual behavior of different PV modules (or PVT collectors). This could also influence the differences in the results.

In case of day type 1, the adapted four-parameter model with $U_{\mathrm{cell-fl}}$-correction underestimates the electrical power

output with a higher $\Delta W_{el}/W_{el,meas}$-value of -2.60 % compared to -0.82 % of Type 835. For day type 2, the $\Delta W_{el}/W_{el,meas}$-value of +0.49 % is slightly better for the adapted four-parameter model with $U_{cell-fl}$-correction than PVT Type 835 (+0.96 %). Nevertheless, in general the PVT Type 835 shows a better overall agreement of the dynamic electrical behavior than the adapted four-parameter model with $U_{cell-fl}$ correction, expressed in the smallest values of $nRMSE_{el}$ for day type 1 (1.77 %) and for day type 2 (3.48 %) compared to the other models.

Tab. 3: Results of the electrical model comparison

Parameter	Unit	PVT A - WISC Type 835		PVT A - WISC four-parameter model, w/ $U_{cell-fl}$-correction		PVT A - WISC four-parameter model, w/o $U_{cell-fl}$-correction	
		Day Type 1	Day Type 2	Day Type 1	Day Type 2	Day Type 1	Day Type 1
MAE_{el}	W	2.34	3.94	6.23	6.38	12.41	14.44
$nMAE_{el}$	-	1.12 %	2.17 %	2.98 %	3.52 %	5.94%	7.97%
$RMSE_{el}$	W	3.71	6.31	6.88	8.18	12.79	15.78
$nRMSE_{el}$	-	1.77 %	3.48 %	3.29 %	4.51 %	6.12%	8.70%
$W_{el,sim}$	kWh	1.037	0.735	1.019	0.732	1.108	0.786
$W_{el,meas}$	kWh	1.046	0.729	1.046	0.729	1.046	0.729
$\Delta W_{el}/W_{el,meas}$	-	-0.82 %	+0.96 %	-2.60 %	+0.49 %	+5.92%	+7.93%

6. Conclusions and outlook

This contribution presented the implementation and validation of an electrical PV performance model in combination with a coupled solar thermal collector model for the simulation of PVT collectors in TRNSYS for three different PVT collectors. Using the identified PVT collector model parameters of the proposed parameter identification process with TRNSYS and GenOpt, the normalized root mean square errors of the model for the thermal part $nRMSE_{th}$ are between 0.67 % and 5.89 % and for the electrical part $nRMSE_{el}$ between 1.39 % and 5.07 %, depending on the day type and PVT collector type. Furthermore, the comparison of the generated energy production shows a good agreement with differences between -0.38% and +2.59 % for the thermal and -0.82 % and +0.98 % for the electrical simulated and measured energy related to the measured values. As a result, the presented study pointed out that the implemented PVT model Type 835 in combination with a solar thermal collector model (e.g. Type 832) as well as the proposed parameter identification procedure are suitable for the modeling of PVT collectors in TRNSYS. In addition, the comparison of the electrical model with a four-parameter (single diode) PV model figured out that the implementation of a four-parameter PV model has no noticeable advantages for the simulation of the electrical power output in case of the analyzed PVT collector types and operating conditions in comparison with the existing performance model. In future work, it is important to further analyze and improve the parameter identification process by the use of different optimization algorithms and cost functions. Furthermore, additional thermal models such as the 2-node-model integrated in Type 832, which calculates the absorber temperature of the PVT collector that is often set as cell temperature, has to be compared to the presented modeling approach. For further model validation it is also important to use a measured long-wave irradiance as model input instead of the described calculation from ambient conditions.

Acknowledgements

This work was part of the research project SolWP-Hybrid. The project was funded by the federal state of Saarland and the European Regional Development Fund (ERDF 2014-2020). The authors are grateful for this support and thank the project partners, Viessmann Heizsysteme GmbH, Sonnenkraft GmbH and DualSun, for their support and cooperation.

References

Almeida, P., Carvalho, M.J., Amorim, R., Mendes, J.F., Lopes, V., 2014. Dynamic testing of systems – Use of TRNSYS as an approach for parameter identification. Solar Energy 104, 60-70. doi:10.1016/j.egypro.2012.11.142

Budig, C., Orozaliev, J., de Keizer, A.C., Kusyy, O., Vajen, K., 2009. Collector parameter identification methods and their uncertainties. In: Proceedings of the ISES Solar World Congress 2009, Johannesburg, South Africa.

Duffie, J.A., Beckman, W.A., 2013. Solar Engineering of Thermal Processes. Fourth edition, John Wiley & Sons, New Jersey, United States of America.

Faiman, D., 2008. Assessing the outdoor operating temperature of photovoltaic modules. Progress in Photovoltaics: Research and Applications 16, 307-315. doi:10.1002/pip.813

Fischer, S., Frey, P., Drück, H., 2012. A comparison between state-of-the-art and neural network modelling of solar collectors. Solar Energy 86, 3268-3277. doi:10.1016/j.solener.2012.09.002

Haller, M., Perers, B., Bales, C., Paavilainen, J., Dalibard, A., Fischer, S., Bertram, E., 2013. TRNSYS Type 832 v5.01, Dynamic Collector Model by Bengt Perers. Updated Input-Output Reference.

Heydenreich, W., Müller, B., Reise, C., 2008. Describing the world with three parameters: a new approach to PV module power modelling. In: Proceedings of the 23rd European Photovoltaic Solar Energy Conference and Exhibition, 2008, Valencia, Spain. doi:10.4229/23rdEUPVSEC2008-4DO.9.4

IEA SHC, 2018. IEA SHC Task 60. PVT Systems: Application of PVT Collectors and New Solutions in HVAC Systems. <http://task60.iea-shc.org/> [Last accessed: 21.08.2018]

ISO 9806, 2013. ISO 9806:2013 Solar energy - Solar thermal collectors - Test methods.

ISO 9806, 2017. ISO 9806:2017 Solar energy - Solar thermal collectors - Test methods. Second edition.

Lämmle, M., Kroyer, T., Fortuin, S., Wiese, M., Hermann, M., 2016. Development and modelling of highly-efficient PVT collectors with low-emissivity coatings. Solar Energy 130, 161-173. doi:10.1016/j.solener.2016.02.007

Lämmle, M., Oliva, A., Hermann, M., Kramer, K., Kramer, W., 2017. PVT collector technologies in solar thermal systems: A systematic assessment of electrical and thermal yields with the novel characteristic temperature approach. Solar Energy 155, 867-879. doi:10.1016/j.solener.2017.07.015

Perers, B., 1997. An improved dynamic solar collector test method for determination of non-linear optical and thermal characteristics with multiple regression. Solar Energy 59, 163-178. doi:10.1016/S0038-092X(97)00147-3

Skoplaki, E., Palyvos, J., 2009. On the temperature dependence of photovoltaic module electrical performance: A review of efficiency/power correlations. Solar Energy 83, 614-624. doi:10.1016/j.solener.2008.10.008

Spirkl, W., 1997. Dynamic System Testing Program Manual. Version 2.7, InSitu Scientific Software.

TRNSYS, 2015. TRNSYS - a Transient System Simulation Program, version 17.02.0005. Solar Energy Laboratory, University of Wisconsin, Madison, Wisconsin, United States of America.

TRNSYS, 2018. TRNSYS - a Transient System Simulation Program, version 18.00.0019. Solar Energy Laboratory, University of Wisconsin, Madison, Wisconsin, United States of America.

Wetter, 2016. GenOpt®. Generic Optimization Program. User Manual. Version 3.1.1, Lawrence Berkeley National Laboratory, University of California, Berkeley, California, United States of America.